

This article was downloaded by:

On: 22 January 2011

Access details: *Access Details: Free Access*

Publisher *Taylor & Francis*

Informa Ltd Registered in England and Wales Registered Number: 1072954 Registered office: Mortimer House, 37-41 Mortimer Street, London W1T 3JH, UK



The Journal of Adhesion

Publication details, including instructions for authors and subscription information:

<http://www.informaworld.com/smpp/title~content=t713453635>

Stress Analysis of *T*-type Butt Adhesive Joint Subjected to External Bending Moments

Toshiyuki Sawa^a; Yuichi Nakano^b; Katsuhiko Temma^c

^a Faculty of Mechanical Engineering, Yamanashi University, Takeda, Kofu, JAPAN ^b Faculty of Mechanical Engineering, Sagami Institute of Technology, Fujisawa-shi, JAPAN ^c Department of Mechanical Engineering, Kisarazu National College of Technology, Kisarazu, Chiba, JAPAN

To cite this Article Sawa, Toshiyuki, Nakano, Yuichi and Temma, Katsuhiko (1987) 'Stress Analysis of *T*-type Butt Adhesive Joint Subjected to External Bending Moments', *The Journal of Adhesion*, 24: 1, 1 – 15

To link to this Article: DOI: 10.1080/00218468708075413

URL: <http://dx.doi.org/10.1080/00218468708075413>

PLEASE SCROLL DOWN FOR ARTICLE

Full terms and conditions of use: <http://www.informaworld.com/terms-and-conditions-of-access.pdf>

This article may be used for research, teaching and private study purposes. Any substantial or systematic reproduction, re-distribution, re-selling, loan or sub-licensing, systematic supply or distribution in any form to anyone is expressly forbidden.

The publisher does not give any warranty express or implied or make any representation that the contents will be complete or accurate or up to date. The accuracy of any instructions, formulae and drug doses should be independently verified with primary sources. The publisher shall not be liable for any loss, actions, claims, proceedings, demand or costs or damages whatsoever or howsoever caused arising directly or indirectly in connection with or arising out of the use of this material.

J. Adhesion, 1987, Vol. 24, pp. 1-15
Photocopying permitted by license only
© 1987 Gordon and Breach Science Publishers, Inc.
Printed in the United Kingdom

Stress Analysis of *T*-type Butt Adhesive Joint Subjected to External Bending Moments

TOSHIYUKI SAWA

Faculty of Mechanical Engineering, Yamanashi University, 4-3-11 Takeda, Kofu, JAPAN

YUICHI NAKANO†

Faculty of Mechanical Engineering, Sagami Institute of Technology, 1-1-25 Nishikaigan Tsujido, Fujisawa-shi 251, JAPAN

KATSUHIRO TEMMA

Department of Mechanical Engineering, Kisarazu National College of Technology, 2-11-1 Kiyomidai-Higashi, Kisarazu, Chiba, JAPAN

(Received July 10, 1986; in final form October 7, 1986)

Stress distributions and displacements at the interface between an adhesive and an adherend are examined when a *T*-type butt adhesive joint, in which two thin plates are joined, is subjected to an external bending moment. In the analyses, general representations of the stresses and the displacements are given using a two-dimensional theory of elasticity in the case where two dissimilar plates are joined. Next, in the case of plates with the same material, effects of Young's modulus of plates to that of an adhesive and the thickness of the adhesive on the stress distribution are made clear by numerical computations. For verification, experiments are performed and an analytical result is in a fairly good agreement with an experimental one.

KEY WORDS Bending moment; butt joint; elasticity; strength design; stress analysis; Young's modulus.

† To whom correspondence regarding this paper should be addressed.

1 INTRODUCTION

With the development of structural adhesives, the use of adhesive bonding is increasing in manufacturing of machine tools and other mechanical structures instead of conventional ways such as bolted, riveted and welded joints.¹⁻³ That is, there are more attractive features as described below in adhesive bonding. 1) stress distribution of a joint becomes almost uniform. 2) joining of different materials is easy. 3) weight of a joint becomes light. 4) absorbing of vibration is feasible due to damping or viscoelastic properties of adhesives and so on. At present, however, in the case of structural adhesive joints, data for designing joints are markedly fewer than those of conventional joints and it is too difficult to estimate the quality of the bonding state of a joint and its durability. On the other hand, mechanical structures are subjected to various types of loads, individually or in a complex way and statically or dynamically, such as tensile, compressive, shearing, bending and torsional loads. It is, therefore, necessary to establish designing and manufacturing methods, as soon as possible, by completing the requisite data such as the stress and the deformation states of structural adhesive joints subjected to each type of load.

Some analytical investigations have been made on the stress distributions of adhesive joints using the finite element method⁴ and theory of elasticity.^{5,6} However, these analyses are done under several assumptions such that the stress or the strain distributes uniformly or linearly in an adhesive, so it seems that the boundary conditions in these adhesive joints are not satisfied sufficiently.

The purpose of this paper is to obtain some fundamental data for strength design of a *T*-type butt adhesive joint as a model of mechanical structures with adhesively bonded joints. In the analysis, the stress distribution and the displacement of this adhesive joint subjected to an external bending moment, in which two dissimilar plates are joined, are examined using a two-dimensional theory of elasticity. Furthermore, in the case of two plates with the same material, the effects of the ratio of Young's modulus of the plates to that of an adhesive, and the thickness of an adhesive, on the stress distribution are made clear by numerical analyses and experiments.

2 THEORETICAL ANALYSIS

Figure 1 shows a model for analysis of a *T*-type butt adhesive joint subjected to an external bending moment M at the top end. Two dissimilar finite thin plates, called the adherend(I) and adherend(III) hereinafter, are joined by the adhesive(II). The length and the height of each adherend are $2l_1, 2h_1, 2l_3$ and $2h_3$, their Young's modulus and Poisson's ratio are E_1, ν_1, E_3 and ν_3 , respectively. Similarly, the thickness of the adhesive is $2h_2$ and its material constants are E_2 and ν_2 . In the present analysis, the bending moment M is substituted for a linearly distributed force $F(x)$ on the top end of the adherend(I) as shown in Figure 1; in

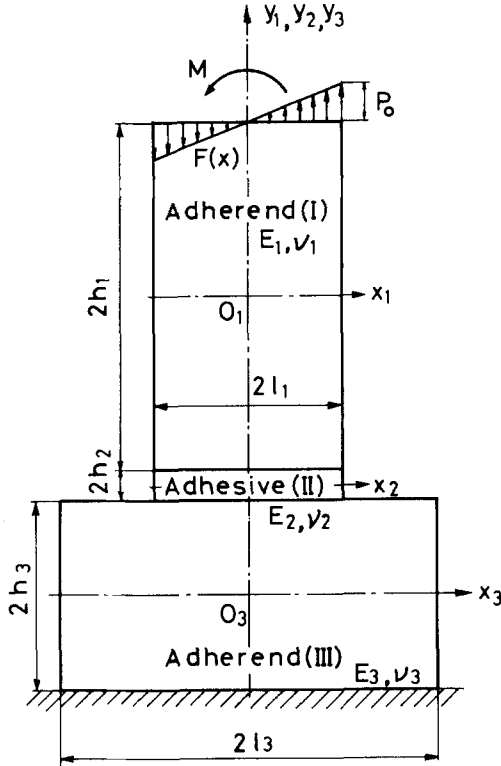


FIGURE 1 Model of *T*-type butt adhesive joint subjected to a bending moment.

addition, the distribution of the force $F(x)$ is expressed by the equation

$$F(x) = P_0 x / l_1 = \sum_{s=1}^{\infty} a_s \sin(2s-1)x / 2l_1$$

using Fourier expansion. Thus, boundary conditions of the joint are expressed as the following equations (1)–(15).

For the adherend(I),

$$\sigma_x^{(I)} = 0 \quad (x_1 = \pm l_1) \quad (1)$$

$$\sigma_y^{(I)} = \sum_{s=1}^{\infty} a_s \sin \frac{2s-1}{2l_1} \pi x \quad (y_1 = h_1) \quad (2)$$

$$\tau_{xy}^{(I)} = 0 \quad (y_1 = h_1) \quad (3)$$

For the adhesive(II),

$$\sigma_x^{(II)} = 0 \quad (x_2 = \pm l_1) \quad (4)$$

For the adherend(III),

$$\sigma_x^{(III)} = 0 \quad (x_3 = \pm l_3) \quad (5)$$

$$\tau_{xy}^{(III)} = 0 \quad (y_3 = -h_3) \quad (6)$$

$$v^{(III)} = 0 \quad (y_3 = -h_3) \quad (7)$$

At the interface between adherend(I) and adhesive(II) ($y_1 = -h_1, y_2 = h_2$),

$$\sigma_y^{(I)} = \sigma_y^{(II)} \quad (-l_1 \leq x_{1,2} \leq l_1) \quad (8)$$

$$\tau_{xy}^{(I)} = \tau_{xy}^{(II)} \quad (-l_1 \leq x_{1,2} \leq l_1) \quad (9)$$

$$\frac{\partial u^{(I)}}{\partial x_1} = \frac{\partial u^{(II)}}{\partial x_2} \quad (-l_1 \leq x_{1,2} \leq l_1) \quad (10)$$

$$v^{(I)} = v^{(II)} \quad (-l_1 \leq x_{1,2} \leq l_1) \quad (11)$$

At the interface between adhesive(II) and adherend(III) ($y_2 = -h_2, y_3 = h_3$),

$$\sigma_y^{(III)} = \begin{cases} 0 & (l_1 < |x_3| < l_3) \\ \sigma_y^{(II)} & (-l_1 \leq x_{2,3} \leq l_1) \end{cases} \quad (12)$$

$$\tau_{xy}^{(III)} = \begin{cases} 0 & (l_1 < |x_3| < l_3) \\ \tau_{xy}^{(II)} & (-l_1 \leq x_{2,3} \leq l_1) \end{cases} \quad (13)$$

$$\frac{\partial u^{(III)}}{\partial x_3} = \frac{\partial u^{(II)}}{\partial x_2} \quad (-l_1 \leq x_{2,3} \leq l_1) \quad (14)$$

$$v^{(III)} = v^{(II)} \quad (-l_1 \leq x_{2,3} \leq l_1) \quad (15)$$

In these equations, $\sigma_x, \sigma_y, \tau_{xy}$ denote the normal and the shear stresses, u and v denote the displacements in x and y directions, respectively. The superscripts (I), (II), and (III) correspond to each adherend and the adhesive, respectively. Using Airy's stress function χ to analyze the stress distribution of the adhesive joint, the stress and the displacement components are expressed by the following equations (16) and (17).

$$\sigma_x = \frac{\partial^2 \chi}{\partial y^2}, \quad \sigma_y = \frac{\partial^2 \chi}{\partial x^2}, \quad \tau_{xy} = -\frac{\partial^2 \chi}{\partial x \partial y} \quad (16)$$

$$\left. \begin{aligned} 2Gu &= -\frac{\partial \chi}{\partial x} + \frac{1}{1+\nu} \frac{\partial \psi}{\partial y} \\ 2Gv &= -\frac{\partial \chi}{\partial y} + \frac{1}{1+\nu} \frac{\partial \psi}{\partial x} \quad (G = E/2(1+\nu)) \end{aligned} \right\} \quad (17)$$

where

$$\nabla^2 \nabla^2 \chi = 0, \quad \nabla^2 \chi = \frac{\partial^2 \psi}{\partial x \partial y}, \quad \nabla^2 \psi = 0 \quad \left(\nabla^2 = \frac{\partial^2}{\partial x^2} + \frac{\partial^2}{\partial y^2} \right)$$

The stress function $\chi^{(I)}$ for the adherend (I) is taken as follows in consideration of the boundary conditions.⁷

$$\begin{aligned} \chi^{(I)} &= \chi_1^{(I)} + \chi_2^{(I)} + \chi_3^{(I)} + \chi_4^{(I)} \\ \chi_1^{(I)} &= \chi_1^{(I)}(\bar{A}_n^I, \bar{B}_s^I, h_1, l_1, \alpha_n^I, \lambda_s^I, \bar{\Delta}_n^I, \bar{\Omega}_s^I, x_1, y_1) \\ \chi_2^{(I)} &= \chi_2^{(I)}(\bar{A}_n^I, \bar{B}_s^I, h_1, l_1, \alpha_n^I, \lambda_s^I, \bar{\Delta}_n^I, \bar{\Omega}_s^I, x_1, y_1) \\ \chi_3^{(I)} &= \chi_3^{(I)}(\bar{A}_n^I, \bar{B}_s^I, h_1, l_1, \alpha_n^I, \lambda_s^I, \bar{\Delta}_n^I, \bar{\Omega}_s^I, x_1, y_1) \\ \chi_4^{(I)} &= \chi_4^{(I)}(\bar{A}_n^I, \bar{B}_s^I, h_1, l_1, \alpha_n^I, \lambda_s^I, \bar{\Delta}_n^I, \bar{\Omega}_s^I, x_1, y_1) \\ \chi_1^{(I)} &= \sum_{n=1}^{\infty} \frac{\bar{A}_n^I}{\bar{\Delta}_n^I \alpha_n^I} [\{ \cosh(\alpha_n^I l_1) + \alpha_n^I l_1 \sinh(\alpha_n^I l_1) \} \sinh(\alpha_n^I x_1) \\ &\quad - \alpha_n^I x_1 \cosh(\alpha_n^I l_1) \cosh(\alpha_n^I x_1)] \cos(\alpha_n^I y_1) \\ &\quad + \sum_{s=1}^{\infty} \frac{\bar{B}_s^I}{\bar{\Omega}_s^I \lambda_s^I} [\{ \sinh(\lambda_s^I h_1) + \lambda_s^I h_1 \cosh(\lambda_s^I h_1) \} \cosh(\lambda_s^I y_1) \\ &\quad - \lambda_s^I y_1 \sinh(\lambda_s^I h_1) \sinh(\lambda_s^I y_1)] \sin(\lambda_s^I x_1) \end{aligned}$$

$$\begin{aligned}
\chi_2^{(I)} &= \sum_{n=1}^{\infty} \frac{\bar{A}_n^I}{\bar{\Delta}_n^I \alpha_n'^{I2}} [\{\cosh(\alpha_n'^I l_1) + \alpha_n'^I l_1 \sinh(\alpha_n'^I l_1)\} \sinh(\alpha_n'^I x_1) \\
&\quad - \alpha_n'^I x_1 \cosh(\alpha_n'^I l_1) \cosh(\alpha_n'^I x_1)] \sin(\alpha_n'^I y_1) \\
&\quad + \sum_{s=1}^{\infty} \frac{\bar{B}_s^I}{\bar{\Omega}_s^I \lambda_s^I} [\{\cosh(\lambda_s^I h_1) + \lambda_s^I h_1 \sinh(\lambda_s^I h_1)\} \sinh(\lambda_s^I y_1) \\
&\quad - \lambda_s^I y_1 \cosh(\lambda_s^I h_1) \cosh(\lambda_s^I y_1)] \sin(\lambda_s^I x_1) \\
\chi_3^{(I)} &= \sum_{n=1}^{\infty} \frac{\bar{A}_n^I}{\bar{\Delta}_n^I \alpha_n'^{I2}} [\{\cosh(\alpha_n'^I l_1) + \alpha_n'^I l_1 \sinh(\alpha_n'^I l_1)\} \sinh(\alpha_n'^I x_1) \\
&\quad - \alpha_n'^I x_1 \cosh(\alpha_n'^I l_1) \cosh(\alpha_n'^I x_1)] \cos(\alpha_n'^I y_1) \\
&\quad - \sum_{s=1}^{\infty} \frac{\bar{B}_s^I}{\bar{\Omega}_s^I \lambda_s^I} \{\lambda_s^I h_1 \sinh(\lambda_s^I h_1) \cosh(\lambda_s^I y_1) \\
&\quad - \lambda_s^I y_1 \cosh(\lambda_s^I h_1) \sinh(\lambda_s^I y_1)\} \sin(\lambda_s^I x_1) \\
\chi_4^{(I)} &= \sum_{n=1}^{\infty} \frac{\bar{A}_n^I}{\bar{\Delta}_n^I \alpha_n'^{I2}} [\{\cosh(\alpha_n^I l_1) + \alpha_n^I l_1 \sinh(\alpha_n^I l_1)\} \sinh(\alpha_n^I x_1) \\
&\quad - \alpha_n^I x_1 \cosh(\alpha_n^I l_1) \cosh(\alpha_n^I x_1)] \sin(\alpha_n^I y_1) \\
&\quad - \sum_{s=1}^{\infty} \frac{\bar{B}_s^I}{\bar{\Omega}_s^I \lambda_s^I} \{\lambda_s^I h_1 \cosh(\lambda_s^I h_1) \sinh(\lambda_s^I y_1) \\
&\quad - \lambda_s^I y_1 \sinh(\lambda_s^I h_1) \cosh(\lambda_s^I y_1)\} \sin(\lambda_s^I x_1)
\end{aligned} \tag{18}$$

where,

$$\begin{aligned}
\alpha_n^I &= \frac{n\pi}{h_1}, \quad \alpha_n'^I = \frac{2n-1}{2h_1} \pi, \quad \lambda_s^I = \frac{2s-1}{2l_1} \pi \\
\bar{\Delta}_n^I &= \sinh(\alpha_n^I l_1) \cosh(\alpha_n^I l_1) - \alpha_n^I l_1 = \bar{\bar{\Delta}}_n^I \\
\bar{\bar{\Delta}}_n^I &= \sinh(\alpha_n'^I l_1) \cosh(\alpha_n'^I l_1) - \alpha_n'^I l_1 = \bar{\Delta}_n^I \\
\bar{\Omega}_s^I &= \sinh(\lambda_s^I h_1) \cosh(\lambda_s^I h_1) + \lambda_s^I h_1 = \bar{\bar{\Omega}}_s^I \\
\bar{\bar{\Omega}}_s^I &= \sinh(\lambda_s^I h_1) \cosh(\lambda_s^I h_1) - \lambda_s^I h_1 = \bar{\Omega}_s^I
\end{aligned}$$

In Eq. (18), \bar{A}_n^I , \bar{B}_s^I , $\bar{\bar{A}}_n^I$, $\bar{\bar{B}}_s^I$, \bar{A}_n^I , \bar{B}_s^I , $\bar{\bar{A}}_n^I$ and $\bar{\bar{B}}_s^I$ ($n, s = 1, 2, 3, \dots$) are undetermined coefficients determined from the boundary conditions. In the same manner, stress functions $\chi^{(II)}$ for the adhesive(II)

and $\chi^{(III)}$ for the adherend(III) are expressed as the Eqs. (19) and (20) by replacing l_1, h_1 with l_1, h_2 and l_3, h_3 in Eq. (18).

$$\chi^{(II)} = \chi_1^{(II)} + \chi_2^{(II)} + \chi_3^{(II)} + \chi_4^{(II)} \tag{19}$$

$$\chi^{(III)} = \chi_1^{(III)} + \chi_2^{(III)} + \chi_3^{(III)} + \chi_4^{(III)} \tag{20}$$

Moreover, undertermined coefficients $\bar{A}_n^I, \bar{B}_s^I, \bar{A}_n^{II}, \bar{B}_s^{II}, \dots, \bar{B}_s^{III}, \bar{A}_n^{III}$ and \tilde{B}_s^{III} ($n, s = 1, 2, 3, \dots$) included in these equations are also determined from the boundary conditions.

Substituting Eqs. (18)–(20) into Eqs. (16) and (17), and equating the obtained results to the boundary conditions (1)–(15), the relationships among undetermined coefficients are written as the following Eqs. (21)–(35), by transforming $\cosh(x), x \sinh(x), \sinh(y), y \cosh(y)$ and so on included in these equations into Fourier series.

$$\left. \begin{aligned} \bar{A}_n^I - \sum_{s=1}^{\infty} \bar{B}_s^I P_{ns}^I = 0, \quad \bar{A}_n^I + \sum_{s=1}^{\infty} \bar{B}_s^I P'_{ns} = 0 \\ \tilde{A}_n^I - \sum_{s=1}^{\infty} \tilde{B}_s^I S_{ns}^I = 0, \quad \tilde{A}_n^I - \sum_{s=1}^{\infty} \tilde{B}_s^I S'_{ns} = 0 \end{aligned} \right\} \tag{21}$$

$$\sum_{n=1}^{\infty} \bar{A}_n^I Q_{ns}^I - \bar{B}_s^I - \sum_{n=1}^{\infty} \tilde{A}_n^I Q'_{ns} - \tilde{B}_s^I = a_s \tag{22}$$

$$\sum_{n=1}^{\infty} \tilde{A}_n^I R_{ns}^I - \tilde{B}_s^I + \sum_{n=1}^{\infty} \tilde{A}_n^I R'_{ns} - \tilde{B}_s^I = 0 \tag{23}$$

$$\left. \begin{aligned} \bar{A}_n^{II} - \sum_{s=1}^{\infty} \bar{B}_s^{II} P_{ns}^{II} = 0, \quad \bar{A}_n^{II} + \sum_{s=1}^{\infty} \bar{B}_s^{II} P'_{ns} = 0 \\ \tilde{A}_n^{II} - \sum_{s=1}^{\infty} \tilde{B}_s^{II} S_{ns}^{II} = 0, \quad \tilde{A}_n^{II} - \sum_{s=1}^{\infty} \tilde{B}_s^{II} S'_{ns} = 0 \end{aligned} \right\} \tag{24}$$

$$\left. \begin{aligned} \bar{A}_n^{III} - \sum_{s=1}^{\infty} \bar{B}_s^{III} P_{ns}^{III} = 0, \quad \bar{A}_n^{III} + \sum_{s=1}^{\infty} \bar{B}_s^{III} P'_{ns} = 0 \\ \tilde{A}_n^{III} - \sum_{s=1}^{\infty} \tilde{B}_s^{III} S_{ns}^{III} = 0, \quad \tilde{A}_n^{III} - \sum_{s=1}^{\infty} \tilde{B}_s^{III} S'_{ns} = 0 \end{aligned} \right\} \tag{25}$$

$$\sum_{n=1}^{\infty} \tilde{A}_n^{III} R_{ns}^{III} - \tilde{B}_s^{III} - \sum_{n=1}^{\infty} \tilde{A}_n^{III} R'_{ns} + \tilde{B}_s^{III} = 0 \tag{26}$$

$$\begin{aligned} \bar{B}_s^{\text{III}} F_s^{\text{III}} - \bar{B}_s^{\text{III}} F_{ns}^{\text{III}} - \sum_{n=1}^{\infty} \bar{A}_n^{\text{III}} H_{ns}^{\text{III}} \\ + \bar{B}_s^{\text{III}} J_s^{\text{III}} + \sum_{n=1}^{\infty} \bar{A}_n^{\text{III}} H'_{ns}{}^{\text{III}} + \bar{B}_s^{\text{III}} J'_{ns}{}^{\text{III}} = 0 \end{aligned} \quad (27)$$

$$\begin{aligned} \sum_{n=1}^{\infty} \bar{A}_n^{\text{I}} Q_{ns}^{\text{I}} - \bar{B}_s^{\text{I}} + \sum_{n=1}^{\infty} \bar{A}_n^{\text{I}} Q'_{ns}{}^{\text{I}} + \bar{B}_s^{\text{I}} \\ - \sum_{n=1}^{\infty} \bar{A}_n^{\text{II}} Q_{ns}^{\text{II}} + \bar{B}_s^{\text{II}} + \sum_{n=1}^{\infty} \bar{A}_n^{\text{II}} Q'_{ns}{}^{\text{II}} + \bar{B}_s^{\text{II}} = 0 \end{aligned} \quad (28)$$

$$\begin{aligned} \sum_{n=1}^{\infty} \bar{A}_n^{\text{I}} R_{ns}^{\text{I}} - \bar{B}_s^{\text{I}} - \sum_{n=1}^{\infty} \bar{A}_n^{\text{I}} R'_{ns}{}^{\text{I}} + \bar{B}_s^{\text{I}} \\ + \sum_{n=1}^{\infty} \bar{A}_n^{\text{II}} R_{ns}^{\text{II}} - \bar{B}_s^{\text{II}} + \sum_{n=1}^{\infty} \bar{A}_n^{\text{II}} R'_{ns}{}^{\text{II}} - \bar{B}_s^{\text{II}} = 0 \end{aligned} \quad (29)$$

$$\begin{aligned} \sum_{n=1}^{\infty} \bar{A}_n^{\text{I}} U_{ns}^{\text{I}} - \bar{B}_s^{\text{I}} V_s^{\text{I}} + \sum_{n=1}^{\infty} \bar{A}_n^{\text{I}} U'_{ns}{}^{\text{I}} - \bar{B}_s^{\text{I}} V_s'{}^{\text{I}} - \bar{B}_s^{\text{I}} W_s^{\text{I}} + \bar{B}_s^{\text{I}} W_s'{}^{\text{I}} \\ - \sum_{n=1}^{\infty} \bar{A}_n^{\text{II}} U_{ns}^{\text{II}} + \bar{B}_s^{\text{II}} V_s^{\text{II}} + \sum_{n=1}^{\infty} \bar{A}_n^{\text{II}} U'_{ns}{}^{\text{II}} - \bar{B}_s^{\text{II}} V_s'{}^{\text{II}} \\ + \bar{B}_s^{\text{II}} W_s^{\text{II}} + \bar{B}_s^{\text{II}} W_s'{}^{\text{II}} = 0 \end{aligned} \quad (30)$$

$$\begin{aligned} \bar{B}_s^{\text{I}} F_s^{\text{I}} - \bar{B}_s^{\text{I}} F_s'{}^{\text{I}} - \sum_{n=1}^{\infty} \bar{A}_n^{\text{I}} H_{ns}^{\text{I}} + \bar{B}_s^{\text{I}} J_s^{\text{I}} + \sum_{n=1}^{\infty} \bar{A}_n^{\text{I}} H'_{ns}{}^{\text{I}} + \bar{B}_s^{\text{I}} J_s'{}^{\text{I}} \\ + \bar{B}_s^{\text{II}} F_s^{\text{II}} + \bar{B}_s^{\text{II}} F_s'{}^{\text{II}} - \sum_{n=1}^{\infty} \bar{A}_n^{\text{II}} H_{ns}^{\text{II}} \\ + \bar{B}_s^{\text{II}} J_s^{\text{II}} - \sum_{n=1}^{\infty} \bar{A}_n^{\text{II}} H'_{ns}{}^{\text{II}} - \bar{B}_s^{\text{II}} J_s'{}^{\text{II}} = 0. \end{aligned} \quad (31)$$

$$\begin{aligned} \sum_{m=1}^{\infty} a_{ms} \left\{ \sum_{n=1}^{\infty} \bar{A}_n^{\text{II}} Q_{nm}^{\text{II}} - \bar{B}_m^{\text{II}} + \sum_{n=1}^{\infty} \bar{A}_n^{\text{II}} Q'_{nm}{}^{\text{II}} + \bar{B}_m^{\text{II}} \right\} \\ - \sum_{n=1}^{\infty} \bar{A}_n^{\text{III}} Q_{ns}^{\text{III}} + \bar{B}_s^{\text{III}} + \sum_{n=1}^{\infty} \bar{A}_n^{\text{III}} Q'_{ns}{}^{\text{III}} + \bar{B}_s^{\text{III}} = 0 \end{aligned} \quad (32)$$

$$\begin{aligned} \sum_{m=1}^{\infty} a_{ms} \lambda_m \left\{ \sum_{n=1}^{\infty} \bar{A}_n^{\text{II}} R_{nm}^{\text{II}} - \bar{B}_m^{\text{II}} - \sum_{n=1}^{\infty} \bar{A}_n^{\text{II}} R'_{nm}{}^{\text{II}} + \bar{B}_m^{\text{II}} \right\} \\ + \lambda_s \left\{ \sum_{n=1}^{\infty} \bar{A}_n^{\text{III}} R_{ns}^{\text{III}} - \bar{B}_s^{\text{III}} + \sum_{n=1}^{\infty} \bar{A}_n^{\text{III}} R'_{ns}{}^{\text{III}} - \bar{B}_s^{\text{III}} \right\} = 0 \end{aligned} \quad (33)$$

$$\begin{aligned} & \sum_{m=1}^{\infty} b_{ms} \left\{ \sum_{n=1}^{\infty} \bar{A}_n^{\text{III}} U_{nm}^{\text{III}} - \bar{B}_m^{\text{III}} V_m^{\text{III}} \sum_{n=1}^{\infty} \bar{A}_n^{\text{III}} U_{nm}^{\text{III}} \right. \\ & \quad \left. + \bar{B}_m^{\text{III}} V_m^{\prime\text{III}} - \bar{B}_m^{\text{III}} W_m^{\text{III}} - \bar{B}_m^{\text{III}} W_m^{\prime\text{III}} \right\} - \sum_{n=1}^{\infty} \bar{A}_n^{\text{II}} U_{ns}^{\text{II}} + \bar{B}_s^{\text{II}} V_s^{\text{II}} \\ & - \sum_{n=1}^{\infty} \bar{A}_n^{\text{II}} U_{ns}^{\prime\text{II}} + \bar{B}_s^{\text{II}} V_s^{\prime\text{II}} + \bar{B}_s^{\text{II}} W_s^{\text{II}} - \bar{B}_s^{\text{II}} W_s^{\prime\text{II}} = 0 \end{aligned} \quad (34)$$

$$\begin{aligned} & \sum_{m=1}^{\infty} b_{ms} \left\{ \bar{B}_m^{\text{III}} F_m^{\text{III}} + \bar{B}_m^{\text{III}} F_m^{\prime\text{III}} - \sum_{n=1}^{\infty} \bar{A}_n^{\text{III}} H_{nm}^{\text{III}} + \bar{B}_m^{\text{III}} J_m^{\text{III}} \right. \\ & \quad \left. - \sum_{n=1}^{\infty} \bar{A}_n^{\text{III}} H_{nm}^{\prime\text{III}} - \bar{B}_m^{\text{III}} J_m^{\prime\text{III}} \right\} + \bar{B}_s^{\text{II}} F_s^{\text{II}} - \bar{B}_s^{\text{II}} F_s^{\prime\text{II}} \\ & - \sum_{n=1}^{\infty} \bar{A}_n^{\text{II}} H_{ns}^{\text{II}} + \bar{B}_s^{\text{II}} J_s^{\text{II}} + \sum_{n=1}^{\infty} \bar{A}_n^{\text{II}} H_{ns}^{\prime\text{II}} + \bar{B}_s^{\text{II}} J_s^{\prime\text{II}} = 0 \end{aligned} \quad (35)$$

where,

$$\begin{aligned} P_{ns}^{\text{I}} &= \frac{4(-1)^{n+s} \lambda_s^1 \alpha_n^{12}}{\bar{\Omega}_s^1 h_1 (\lambda_s^{12} + \alpha_n^{12})^2} \sinh^2(\lambda_s^1 h_1) \\ P_{ns}^{\prime\text{I}} &= \frac{4(-1)^{n+s} \lambda_s^1 \alpha_n^{\prime 12}}{\bar{\Omega}_s^1 h_1 (\lambda_s^{12} + \alpha_n^{\prime 12})^2} \cosh^2(\lambda_s^1 h_1) \\ S_{ns}^{\text{I}} &= \frac{4(-1)^{n+s} \alpha_n^{\prime 13}}{\bar{\Omega}_s^1 h_1 (\lambda_s^{12} + \alpha_n^{\prime 12})^2} \cosh^2(\lambda_s^1 h_1) \\ S_{ns}^{\prime\text{I}} &= \frac{4(-1)^{n+s} \alpha_n^{13}}{\bar{\Omega}_s^1 h_1 (\lambda_s^{12} + \alpha_n^{12})^2} \sinh^2(\lambda_s^1 h_1) \\ Q_{ns}^{\text{I}} &= \frac{4(-1)^{n+s} \lambda_s^{12} \alpha_n^1}{\bar{\Delta}_n^1 l_1 (\lambda_s^{12} + \alpha_n^{12})^2} \cosh^2(\alpha_n^1 l_1) \\ Q_{ns}^{\prime\text{I}} &= \frac{4(-1)^{n+s} \lambda_s^{12} \alpha_n^{\prime 1}}{\bar{\Delta}_n^1 l_1 (\lambda_s^{12} + \alpha_n^{\prime 12})^2} \cosh^2(\alpha_n^{\prime 1} l_1) \\ R_{ns}^{\text{I}} &= \frac{4(-1)^{n+s} \lambda_s^1 \alpha_n^{\prime 12}}{\bar{\Delta}_n^1 l_1 (\lambda_s^{12} + \alpha_n^{\prime 12})^2} \cosh^2(\alpha_n^{\prime 1} l_1) \\ R_{ns}^{\prime\text{I}} &= \frac{4(-1)^{n+s} \lambda_s^1 \alpha_n^{12}}{\bar{\Delta}_n^1 l_1 (\lambda_s^{12} + \alpha_n^{12})^2} \cosh^2(\alpha_n^1 l_1) \end{aligned}$$

$$H_{ns}^I = \frac{2(-1)^{n+s} \cosh^2(\alpha_n^I l_1)}{2G_1 \bar{\Delta}_n^I l_1 (\lambda_s^{I2} + \alpha_n^{I2})} \left\{ \frac{\nu - 1}{1 + \nu} + \frac{\alpha_n^{I2} - \lambda_s^{I2}}{\alpha_n^{I2} + \lambda_s^{I2}} \right\}$$

$$H_{ns}'^I = \frac{2(-1)^{n+s} \cosh^2(\alpha_n^I l_1)}{2G_1 \bar{\Delta}_n^I l_1 (\lambda_s^{I2} + \alpha_n^{I2})} \left\{ \frac{\nu - 1}{1 + \nu} + \frac{\alpha_n^{I2} - \lambda_s^{I2}}{\alpha_n^{I2} + \lambda_s^{I2}} \right\}$$

$$F_s^I = \frac{2}{E_1 \lambda_s^I \bar{\Omega}_s^I} \sinh^2(\lambda_s^I h_1)$$

$$F_s'^I = \frac{2}{E_1 \lambda_s^I \bar{\Omega}_s^I} \cosh^2(\lambda_s^I h_1)$$

$$J_s^I = \frac{1}{2G_1 \lambda_s^I \bar{\Omega}_s^I} \left\{ \lambda_s^I h_1 + \frac{\nu - 1}{1 + \nu} \sinh(\lambda_s^I h_1) \cosh(\lambda_s^I h_1) \right\}$$

$$J_s'^I = \frac{1}{2G_1 \lambda_s^I \bar{\Omega}_s^I} \left\{ \lambda_s^I h_1 - \frac{\nu - 1}{1 + \nu} \sinh(\lambda_s^I h_1) \cosh(\lambda_s^I h_1) \right\}$$

$$U_{ns}^I = \frac{2\alpha_n^I (-1)^{n+s} \cosh^2(\alpha_n^I l_1)}{2G_1 \bar{\Delta}_n^I l_1 (\lambda_s^{I2} + \alpha_n^{I2})} \left\{ \frac{\nu - 1}{1 + \nu} - \frac{\alpha_n^{I2} - \lambda_s^{I2}}{\alpha_n^{I2} + \lambda_s^{I2}} \right\}$$

$$U_{ns}'^I = \frac{2\alpha_n^I (-1)^{n+s} \cosh^2(\alpha_n^I l_1)}{2G_1 \bar{\Delta}_n^I l_1 (\lambda_s^{I2} + \alpha_n^{I2})} \left\{ \frac{\nu - 1}{1 + \nu} - \frac{\alpha_n^{I2} - \lambda_s^{I2}}{\alpha_n^{I2} + \lambda_s^{I2}} \right\}$$

$$V_s^I = \frac{1}{2G_1 \bar{\Omega}_s^I} \left\{ \lambda_s^I h_1 + \frac{\nu - 1}{1 + \nu} \sinh(\lambda_s^I h_1) \cosh(\lambda_s^I h_1) \right\}$$

$$V_s'^I = \frac{1}{2G_1 \bar{\Omega}_s^I} \left\{ \lambda_s^I h_1 - \frac{\nu - 1}{1 + \nu} \sinh(\lambda_s^I h_1) \cosh(\lambda_s^I h_1) \right\}$$

$$W_s^I = \frac{2}{E_1 \bar{\Omega}_s^I} \cosh^2(\lambda_s^I h_1)$$

$$W_s'^I = \frac{2}{E_1 \bar{\Omega}_s^I} \sinh^2(\lambda_s^I h_1)$$

$$a_{ms} = \frac{1}{l_3} \left\{ \frac{\sin(\lambda_m^{\text{II}} - \lambda_s^{\text{III}}) l_2}{\lambda_m^{\text{II}} - \lambda_s^{\text{III}}} - \frac{\sin(\lambda_m^{\text{II}} + \lambda_s^{\text{III}}) l_2}{\lambda_m^{\text{II}} + \lambda_s^{\text{III}}} \right\}$$

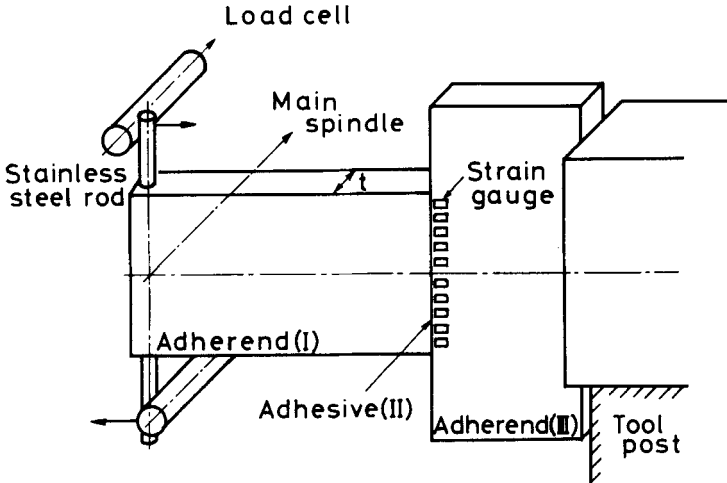
$$b_{ms} = \frac{1}{l_2} \left\{ \frac{\sin(\lambda_m^{\text{III}} - \lambda_s^{\text{II}}) l_2}{\lambda_m^{\text{III}} - \lambda_s^{\text{II}}} - \frac{\sin(\lambda_m^{\text{III}} + \lambda_s^{\text{II}}) l_2}{\lambda_m^{\text{III}} + \lambda_s^{\text{II}}} \right\}$$

In computations, infinite terms of the series with respect to n and

s in Eqs. (21)–(35) are taken as finite terms N , i.e. $24 \times N$ simultaneous equations with undetermined coefficients $\bar{A}_n^I, \bar{B}_n^I, \bar{A}_n^{\bar{I}}, \bar{B}_s^{\bar{I}}, \dots, \bar{A}_n^{III}, \bar{B}_s^{III}, \bar{A}_n^{\bar{III}}$ and $\bar{B}_s^{\bar{III}}$ are obtained. These undetermined coefficients are determined by solving the above equations. Finally, the stress and the displacement distributions are obtained using the determined coefficients.

3 EXPERIMENTAL METHOD

Figure 2 shows an experimental setup and dimensions of the joint in which two adherends with the same material are joined. It is seen from the figure that the thickness t of adherends is very thin compared with the other dimensions. This reason is that the analysis of the adhesive joint can then be done under a generalized plane stress state. The material of the adherends is structural steel (S45C, JIS) and that of the adhesive is a type of epoxy resin, Scotch-Weld 1838 B/A (SUMITOMO 3M Co. Ltd.). The bonding surface of



$$\begin{aligned}
 2h_1 &= 100, & 2l_1 &= 50 \\
 2h_2 &= 0.05, & 2l_3 &= 100 \\
 2h_3 &= 50, & t &= 7.2 \text{ (mm)}
 \end{aligned}$$

FIGURE 2 Sketch of experimental setup.

each adherend is finished by grinding and degreased by acetone prior to bonding. The adhesive joints are cured at 65°C for 24 hours. Twelve strain gauges (gauge length is 0.3 mm) are attached to the adherends as close as possible to the interface of the adhesive. An opposite end to the bonded surface of the adherend(III) is mounted tightly on the tool post of a lathe. A bending moment is applied through a stainless steel rod inserted in a through hole of the adherend(I), and detected by a load cell, which is especially made for the experiment and mounted to the main spindle of the lathe. The normal stresses of the interface in the adherend are picked up by the strain gauges and the output signals are recorded by an oscillograph through dynamic strain amplifiers.

4 NUMERICAL RESULTS AND COMPARISONS WITH EXPERIMENTAL ONES

4.1 Numerical results

Numerical computations are carried out with the same dimensions of the adhesive joint as those used in the experiment shown in Figure 2. In computations, the number of terms N of the series is taken as 100, which is checked to obtain the stresses and the displacements with satisfactory accuracy. Figures 3 and 4 show effects of the ratio E_1/E_2 of Young's modulus of the adherend to that of the adhesive

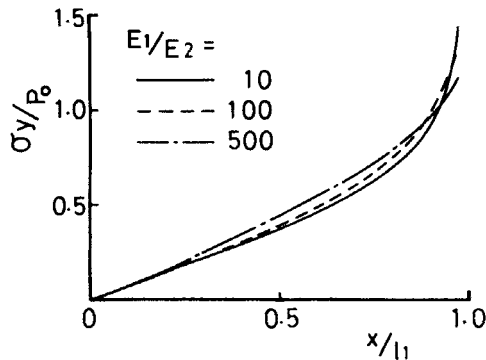


FIGURE 3 Effects of the ratio of Young's modulus of adherend to that of adhesive on the normal stress distribution. ($2h_1 = 100$ mm, $2h_2 = 0.05$ mm, $2h_3 = 50$ mm).

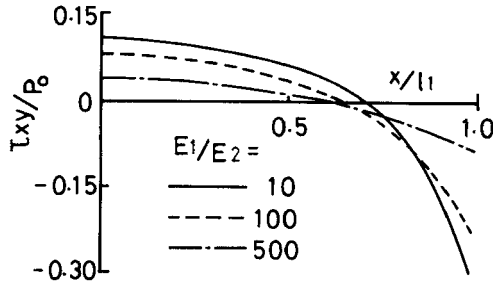


FIGURE 4 Effects of the ratio of Young's modulus of adherend to that of adhesive on the shear stress distribution. ($2h_1 = 100$ mm, $2h_2 = 0.05$ mm, $2h_3 = 50$ mm).

on the normal and the shear stresses at the interface between the adhesive and the adherends. Also, the effects of the thickness of the adhesive on each stress are shown in Figures 5 and 6. In these figures, the abscissa is the ratio of the distance from the center of the adherend in the x -direction to the half length l_1 of the adherend(I) and the ordinate is the ratio of the normal or the shear stress to the stress P_0 shown in Figure 1. The normal or the shear stress distributions of the adherends and the adhesive in y_1 , y_2 and y_3 -directions can be calculated from the present analysis.

From Figures 3 and 4, with a decrease of the ratio E_1/E_2 , it is seen that the singularities of the normal and the shear stresses become large at the end of the interface between the adhesive and the adherend, *i.e.*, $x/l_1 = 1.0$.⁸ With regard to the effect of the

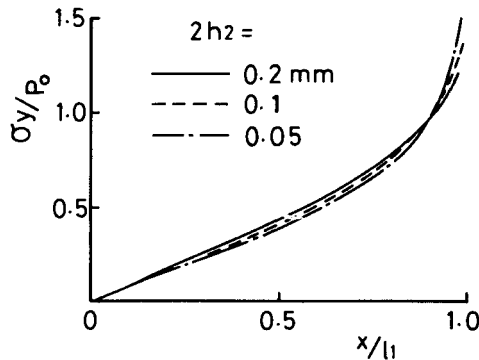


FIGURE 5 Effects of thickness of adhesive on the normal stress distribution. ($2h_1 = 100$ mm, $2h_3 = 50$ mm, $E_1/E_2 = 100$).

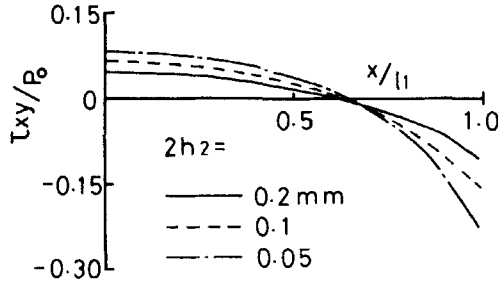


FIGURE 6 Effects of thickness of adhesive on the shear stress distribution. ($2h_1 = 100$ mm, $2h_3 = 50$ mm, $E_1/E_2 = 100$).

adhesive thickness $2h_2$, it is seen from Figures 5 and 6 that the singularities of both the stresses become large at the end of the interface with a decrease of the thickness $2h_2$.

4.2 Comparison with Respect to the Normal Stress

Figure 7 shows the comparison of a numerical result with an experimental one with respect to the normal stress distribution at the position where strain gauges are mounted and at the interface

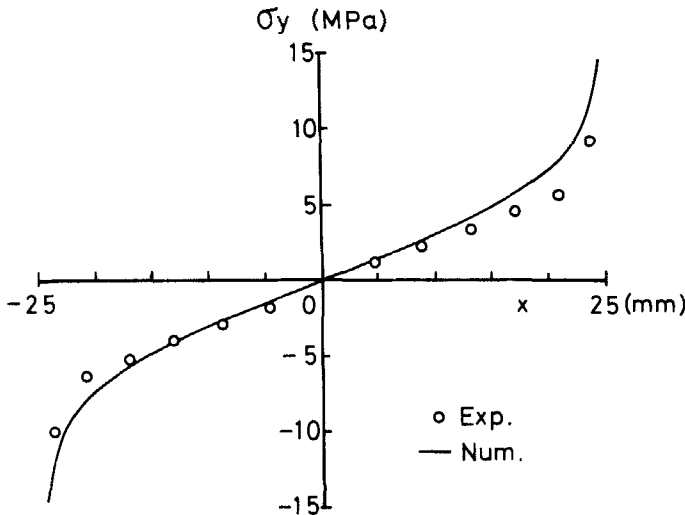


FIGURE 7 Comparison between numerical and experimental results in the case where the bending moment is 29.4 N-m.

between the adhesive(II) and the adherend(III) (solid line) when the external bending moment of $29.4 N\cdot m$ is applied. In this computation, Young's modulus and Poisson's ratio of the adhesive and those of the adherend are 3.33 GPa, 0.34, 206 GPa and 0.3, respectively. The abscissa is the distance from the center of the adherend in the x -direction. From the figure, it seems that the numerical result is in a fairly good agreement with the experimental one.

5 CONCLUSIONS

The present paper deals with a stress analysis of a T -type butt adhesive joint subjected to an external bending moment and discussion is made on some mechanical characteristics of the joint from theoretical analyses and experiments.

Results obtained are as follows :

1) Stress distribution and displacement of the joint, in which two dissimilar plates are joined, are analyzed using a two-dimensional theory of elasticity.

2) In the case of two plates with the same material, effects of the ratio of Young's modulus of the plates to that of an adhesive, and the thickness of the adhesive, on the stress distribution are made clear by numerical computations.

3) Normal stress distribution at the interface between the adhesive and the adherend is measured experimentally. It is shown that the numerical result is in a fairly good agreement with the experimental one.

References

1. H. I. Chowdhury, M. M. Sadek and S. A. Tobias, *Proc. 15th M.T.D.R. Conf.*, 1974, pp. 237.
2. E. J. Lamb and K. Al-Timimi, *Proc. 18th M.T.D.R. Conf.*, 1977, pp. 561.
3. S. M. Robie, *12th North American Manufacturing Research Conf. Proc.*, SME, 1984, pp. 487.
4. R. D. Adams, J. Coppedale and N. A. Peppiatt, *J. Strain Analysis* **13**, 1 (1978).
5. J. L. Lubkin, *J. Applied Mechanics* **24**, 255 (1957).
6. T. Wah, *Int. J. Mechanical Science* **18**, 223 (1976).
7. S. P. Timoshenko and J. N. Goodier, *Theory of Elasticity* (McGraw-Hill, New York, 1970), 3rd ed.
8. J. K. Sen and R. M. Jones, *AIAA Jour.* **18**, 1376 (1980).